12

Human Perceived Transparency with Time Delay

Sandra Hirche[1] and Martin Buss[2]

[1] Tokyo Institute of Technology
Fujita Lab, Dept. of Mechanical and Control Engineering
152-8552 Tokyo, Japan*
S.Hirche@ieee.org
[2] Technische Universität München
Institute of Automatic Control Engineering
D-80290 Munich, Germany
M.Buss@ieee.org

Summary. Transparency – in the sense that the technical systems and communication network should not be felt by the human – is one of the key issues in telerobotics control design. The communication characteristics is one of the crucial factors for the achievable transparency level in bilateral telerobotic control architectures. Especially time delay – resulting from the communication network between the operator site and the tele-robot – deteriorates the realistic (transparent) perception of the remote environment. The quantitative analysis of the time delay influences on transparency is the major goal of this chapter. Technical measures along with human haptic perception characteristics play a key role when evaluating transparency. The guiding questions for this chapter are: how does constant time delay modify the mechanical properties displayed to the human, and can the human perceive this distortion or not. The mass, spring, and damper characteristics as displayed to the human are derived as function of the time delay and the environment parameters. Known psychophysical facts are applied to analyze and interpret the results from a human perception point of view. The results are validated in simulations, experiments, and human user studies.

12.1 Introduction

The communication between the operator side with the multi-modal human system interface and the remote side with the telerobot typically takes place over a communication network as depicted in Fig. 12.1. As a result the motion and force signals arrive delayed at the corresponding receiver side. In terrestial telerobotics application the transmission time delay is typically in the range of some milliseconds up to several hundred milliseconds depending on distance and communication infrastructure; in space application the data transmission may easily take several seconds. Time delay in the haptic feedback loop represents one of the key challenges in control design with respect to stability and transparency. Without appropriate control measures even small time delay may destablize the telerobotic system [1] resulting in a severe hazard to the safety of the human and the remote environment. The wave variable (scattering)

* This research has been performed while the first author was with the Institute of Automatic Control Engineering, Technische Universität München, D-80290 Munich, Germany.

M. Ferre et al. (Eds.): Advances in Telerobotics, STAR 31, pp. 191–209, 2007.
springerlink.com

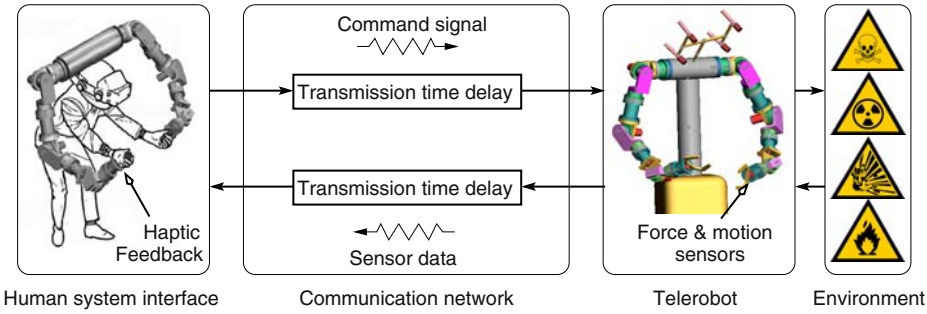

Fig. 12.1. Telerobotic system with transmission time delay

transformation introduced in Sec. 10.4 represents one of the most prominent control approaches to stabilize the telerobotic system with time delay, see also [2, 3]. Stability is guaranteed for arbitrarily large constant time delay. Nevertheless, the time delay value has a significant influence on transparency.

Transparency – in the sense that the technical systems and communication network should not be felt by the human, i.e. the operator should feel as if directly being present and active in the remote environment – is aside from stability one of the key issues in telerobotic systems. Ideally, the human operator feels as if directly interacting with the (remote) task [4]. This is expressed in transparency criteria requiring that mechanical properties of the environment are exactly transmitted to the human operator, motion and forces at the master and the slave device should be equal [5, 6]. Naturally, there is a trade-off between transparency and robust stability in all control schemes, i.e. ideal transparency is not achievable in real systems [5, 7, 8]. Transparency further deteriorates in telerobotic systems with time delay as the bandwidth of the closed loop system has to be severely reduced in order to achieve stability [9]. If the time delay between operator action and the corresponding haptic feedback is too large the telerobotic systems becomes inoperable. Nevertheless, direct haptic feedback is still beneficial for task completion even with a significant time delay of up to one second as experimentally validated in [10, 11]. Other typical communication effects like time-varying delay and the loss of data additionally influence stability and transparency, but are beyond the scope of this chapter. For control architectures considering time-varying delay refer to [12, 13, 14, 15, 16, 17] and for packet loss to [18, 19, 20, 21]. A transparency analysis considering communication effects can be found in [22].

Main focus in this chapter is on *how* constant time delay and the tuning of the control influence the human perception of the remote environment. The *feel* of the human is essential, hence, the consideration of human factors is an important issue for transparency evaluation. The transparency measures known from the literature, such as the maneuverability index [6], impedance error norms [23], or the Z-width [24] are well-suited for the comparison of control schemes in technical terms. However, the interpretation considering human factors is difficult. One of the main contributions of this chapter is a time delay transparency analysis from a human haptic perception point of view using methods and results from psychophysics. Humans may not discriminate arbitrarily small differences in a physical quantity, expressed by the *just noticeable difference*

(JND). Numerous psychophysical studies on the JND of mechanical impedance parameters, such as stiffness [25, 26], inertia [27], and viscosity [27, 28], exist. These results are applied in the transparency evaluation on the basis of a comparison between the mechanical parameters of the impedance transmitted to the human operator and of the real environment impedance. Exemplarily, the widely used wave (scattering) variable control approach, see Sec. 12.4 and [2, 3] for details, is considered in the analysis. For a comparison of other control schemes using a similar approach refer to [29]. Using a low frequency approximative analysis based on a Padé first order model for the time delay it is shown that environment mechanical parameters are distorted by communication time delay and the wave (scattering) variable approach, i.e. a) in free space motion communication time delay introduces artificial inertia; b) stiff environments are displayed softer; c) displayable stiffness is upper bounded; d) environment stiffness discrimination is limited; e) as a result there is a detection threshold for relative changes in time delay. The results are analyzed from a human perception point of view using psychophysical insights of JNDs for mechanical parameters; design issues are discussed. The results are validated in experiments and human user studies. The remainder of this chapter is organized as follows: in Section 2 transparency measures and psychophysical aspects are reviewed. Section 3 provides the objective transparency analysis followed by a perception oriented analysis in Section 4 and design issues in Section 5. Experimental validation results are presented in Section 5.

12.2 Background

In the following the state of the art in transparency analysis and the psychophysical results, related to this work are briefly reviewed. Further the assumptions for the subsequent analysis are clarified.

12.2.1 Transparency

The telerobotic system design goal is that the human cannot distinguish between direct interaction with an environment and teleoperated interaction with an remote environment. Then the system is called *transparent*. Ideally the human feels as if directly performing the task in the (remote) environment [4]. According to [6] a system is transparent if the positions and forces at master and slave device are equal, i.e. $x_h = x_e$ and $f_h = f_e$. The derived transparency measure, called maneuverability, comprises two values based on the integral norm in the frequency domain for the transfer functions in operator force to position error and operator force to force error, respectively. Small values indicate a good level of transparency. Alternatively, in [5] for transparency the equality of the impedance transmitted to the human operator and the environment impedance is required

$$Z_t = Z_e, \tag{12.1}$$

see Fig. 12.2 for a visualization of these impedances. Measures derived from this criterion are integral impedance error norms in the frequency domain as applied in [23] and the Z-width [24], which expresses the dynamic range of the impedance transmitted to the operator. It is quantified for the two extreme values of environment impedance $Z_e = 0$

(free space motion) and $Z_e \to \infty$ (infinitely stiff wall). Accordingly, transparency is good if $Z_t \to 0$ and $Z_t \to \infty$, respectively. All mentioned transparency measures are well-suited for the qualitative comparison of control schemes, however, a direct relation of the obtained values to psychophysical findings and such the interpretation using human haptic perception characteristics is difficult.

12.2.2 Human Haptic Perception

The level of transparency, according to the transparency definition, can be interpreted as the human perceived performance of the telerobotic control system. Hence the *feel* of the human is essential for transparency evaluation. To measure this *feel* depending on physical stimuli is the goal of psychophysics, which is the branch of psychology concerned with the quantitative relation between physical stimuli and the sensations and perceptions evoked by these stimuli, see [30] for a comprehensive introduction.

It is well known that the human cannot discriminate arbitrarily small differences in a physical quantity, expressed by the *just noticeable difference* (JND), the smallest difference in a sensory input that is perceivable by a human being. For many sensory modalities the JND is an increasing function of the base level of input. For most force-related physical properties the ratio of the two is roughly constant over a large range [31] and can therefore be represented by Weber's law [32]

$$\frac{\Delta I}{I} = c, \tag{12.2}$$

where I is the original intensity of stimulation, ΔI is the addition to it required for the difference to be perceivable, and c is the Weber fraction. Discrimination thresholds for mechanical parameters such as stiffness, inertia, and viscosity are typically given as the percentual change with respect to the original intensity of stimulation. Accordingly, we will refer to the percentual discrimination threshold as JND in this chapter. Some of the most relevant JNDs for haptic telerobotic systems are summarized in Table 12.1.

Remark 1. It is well known that the experimental conditions have a significant influence on the results gained in psychophysical experiments. This explains the in some cases wide variation for JNDs. Additionally, some parameters, as e.g. inertia, are suspected of not [33] following Weber's law given by (12.2). As the results are empirically obtained, they generally represent a statistical quantity, i.e. individual differences exist.

Table 12.1. Perceptual discrimination thresholds (JND) for haptics related properties

Physical property	JND [%]	Experimental conditions
Stiffness	23 ± 3 [25]	arm/forearm, cross-limb-matching
	8 [26]	pinch-fingers, work/maximum force applied
Viscosity	34 ± 5 [28]	arm/forearm, cross-limb-matching, > 20 Ns/m
	13.6 ± 3 [27]	pinch-fingers, at 120 Ns/m
Inertia	21 ± 3.5 [27]	pinch-fingers, at 12 kg

12.2.3 Assumptions

For discussion simplicity the following assumptions are made for the subsequent transparency analysis:

A1 A telerobotic system with one degree of freedom (1DoF) is assumed, with the master and the slave device being kinematically similar. An extension of the proposed approach to the more general case is straightforward if the cartesian directions in the master and the slave device are dynamically decoupled which can be achieved by appropriate local control.

A2 The slave device is assumed to be controlled such that its own dynamics is negligible, i.e. the slave device velocity is equal to the desired slave device velocity $v_s = v_e = v_s^d$, see Fig. 12.1. The same assumption is made for the master device, such that the force displayed to the human is equal to the desired master force $f_h = f_h^d$. The extension to the case with non-negligible master and slave dynamics is discussed later in this chapter for the 1DoF case. The extension to multi-DoF devices with non-negligible dynamics is straightforward in the case of decoupled cartesian directions which can be achieved by appropriate local control.

A3 Assume that the environment impedance Z_e can be approximated by a linear time-invariant (LTI) system, which is valid for most considered environments. The environment impedance can then be represented by the transfer function $Z_e(s) = f_e(s)/v_e(s)$ with $s = \sigma + j\omega$ denoting the Laplace variable.

A4 The time delays T_1, T_2 in the forward and backward path, respectively are assumed to be constant and arbitrarily large.

A5 The wave (scattering) variable control approach is applied to stabilize the overall telerobotic system in the presence of constant time delay, see Sec. 12.4 and [2, 3] for details.

12.3 Transparency Analysis

The existence of JND results for mechanical impedance parameters such as stiffness, damping, and inertia encourage a transparency evaluation based on the comparison of the parameters of the impedance displayed to the human and the real environment impedance. Another advantage is that the analysis can conveniently be performed in the frequency domain. The goal is to derive the displayed stiffness, damping and inertia depending on the time delay value. Therefore the displayed impedance Z_t is expressed as function of the round-trip time delay $T = T_1 + T_2$ and the environment impedance Z_e. Straightforward manipulation of the equations for the wave (scattering) variable transformation (10.12)with $f_m = f_h$, $v_m = v_h$ using assumptions A1-A5 yields

$$Z_t(s) = b\frac{1 + R(s)\, e^{-sT}}{1 - R(s)\, e^{-sT}} \quad \text{with} \quad R(s) = \frac{Z_e(s) - b}{Z_e(s) + b}, \tag{12.3}$$

where $b > 0$ represents the wave impedance, the parameter of the wave (scattering) variable transformation. Note that for zero time delay $T = 0$ the displayed impedance is equal to the environment impedance, meaning ideal transparency in the sense of (12.1). For non-zero time delay the displayed and environment impedance differ in general.

Due to the delay element the transfer function has an infinite number of poles and zeros rendering the interpretation of the displayed impedance as simple mass-spring-damper system difficult. Therefore, the transfer function from (12.3) is approximated by a lower order system.

12.3.1 Analytical Low Frequency Approximation

The approximation of the displayed impedance transfer function is derived employing the commonly used Padé series of finite order to approximate the delay transfer functions e^{-sT} in (12.3). The order of the displayed impedance approximation depends on the order N of the Padé approximation. A Padé approximation of order N is valid for frequencies $\omega < N/(3T)$. In order to simplify the analysis the time delay element is approximated here by a first order, i.e. $N = 1$, Padé series

$$e^{-sT} \approx \frac{1 - \frac{T}{2}s}{1 + \frac{T}{2}s}. \tag{12.4}$$

This comes at the cost that for large round-trip time delay the approximation validity range does not fully cover the frequency range of human proprioreceptive and kinesthetic perception (up to approximately 60 Hz). Inserting (12.4) in (12.3) yields the approximated displayed impedance

$$Z_t(s) \approx Z_t^{\text{app}}(s) = b\frac{2Z_e(s) + bTs}{2b + TsZ_e(s)} \tag{12.5}$$

In accordance to the limited frequency range of approximation validity for further analysis this transfer function is split into a low frequency component $Z_{t,lf}^{\text{app}}$ and a high frequency component F_{hf}

$$Z_t^{\text{app}}(s) = Z_{t,lf}^{\text{app}}(s)F_{hf}(s) \tag{12.6}$$

with the high frequency component having approximately unity gain at lower frequencies. The component $Z_{t,lf}^{\text{app}}$ represents a good approximation of the low frequency behavior of the displayed impedance. The mechanical parameters of the approximated displayed impedance $Z_{t,lf}^{\text{app}}$ can be derived analytically as a function of the round-trip time delay T, the wave impedance b, and the environment impedance Z_e, which is exemplarily carried out in detail for the prototypical cases *free space motion* and *contact with a stiff wall*.

12.3.2 Analysis for Prototypical Environment Impedances

Free Space Motion

In free space motion, no environment force is exerted on the telerobot $f_e = 0$, i.e. the environment impedance is $Z_e = 0$. The exact displayed impedance (12.3) is

$$Z_t(s) = b\frac{1 - e^{-sT}}{1 + e^{-sT}}. \tag{12.7}$$

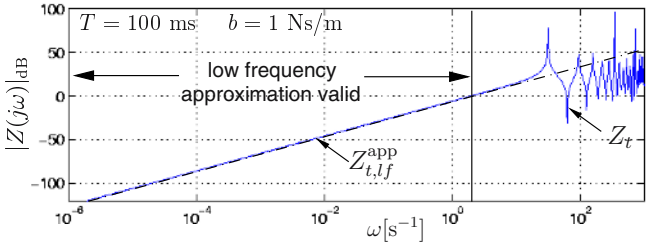

Fig. 12.2. Amplitude/frequency characteristics of the exact and the approximated displayed impedance in *free space motion*

Inserting the environment impedance into (12.5) gives the approximation of the displayed impedance valid for low frequencies

$$Z_t^{\mathrm{app}}(s) = m_t s \frac{1}{1 + \frac{T}{2}s}. \tag{12.8}$$

with

$$m_t = \frac{bT}{2}. \tag{12.9}$$

The lefthand part sm_t in (12.8) represents the dominant low frequency component $Z_{t,lf}^{\mathrm{app}}$ from (12.6). The righthand factor is the high frequency component F_{hf} satisfying $|F_{hf}(0)| = 1$. The similarity of the exact and the approximated displayed impedance for low frequencies can also be observed from their frequency responses for a simulated example, see Fig. 12.2. The displayed impedance is an inertia with the mass m_t (12.9). A similar result is presented for the static case in [34], its validity is extended here to a low frequencies.

Contact with a Stiff Wall Environment

In contact with a stiff wall, a force proportional to the wall penetration depth with the stiffness k_e acts on the teleoperator; the environment impedance is described by the transfer function $Z_e = k_e/s$. The exact displayed impedance (12.3) is

$$Z_t(s) = b\frac{k_e + bs + (k_e - bs)e^{-sT}}{k_e + bs - (k_e - bs)e^{-sT}}. \tag{12.10}$$

The approximation (12.5) of the displayed impedance for low frequency is analogously computed to the *free space motion* case

$$Z_t^{\mathrm{app}}(s) = \frac{k_t}{s}\left(1 + \frac{bT}{2k_e}s^2\right) \tag{12.11}$$

with

$$\frac{1}{k_t} = \frac{1}{k_e} + \frac{T}{2b}. \tag{12.12}$$

The lefthand factor $Z_{t,lf}^{\mathrm{app}} = k_t/s$ is the low frequency component from (12.6). The right hand factor in (12.11) exhibits high pass behavior satisfying $|F_{hf}(0)| = 1$. A simulation

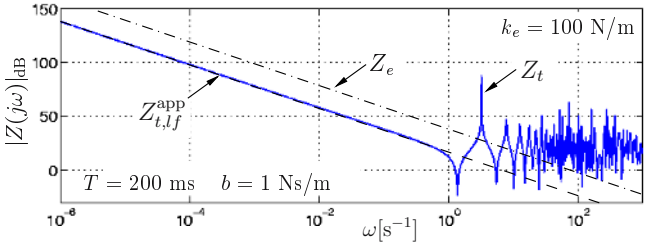

Fig. 12.3. Amplitude/frequency characteristics of the exact and the approximated displayed impedance in *contact with a stiff wall*

example in Fig. 12.3 shows the frequency responses for the exact and the approximated displayed impedance, which are similar at low frequencies. The displayed impedance in *contact with a stiff wall* exhibits a springlike behavior at low frequencies, however, with a lower stiffness k_t than the environment stiffness k_e, see also Fig. 12.3. As observable from (12.12), the communication subsystem including the wave (scattering) variable transformation can be interpreted as a rod with a stiffness coefficient $2b/T$ in mechanical series connection with the environment.

12.4 Perception Oriented Time Delay Transparency Analysis

On the basis of the above analysis and taking into account relative human perception limitations we obtain the following insights along with design guidelines for bilateral telerobotic systems.

12.4.1 Communication Induced Inertia Perception

In *free space motion* an inertia is displayed to the human operator even though no inertia is contained in the environment. The inertia characteristics is induced by the wave (scattering) variable transformation and the communication delay. With increasing round-trip time delay T and wave impedance b the displayed inertia m_t proportionally grows (12.9) as shown in a simulation example in Fig. 12.4. Given a time delay $T > 0$, free space motion is transparent in the sense of (12.1), i.e. $m_t = 0$, only if $b = 0$ which is unfeasible in terms of the tuning requirement $b > 0$. Considering human perception, an inertia is not perceivable if it is below the absolute human perception threshold Δm for inertia.

Example 1. Lets assume free space motion of the slave device, a communication round-trip delay $T = 200$ ms, typical for the communication over the Internet, and the wave impedance tuned to $b = 1$ Ns/m. Then the operator feels an inertia $m_t = 0.1$ kg. If the wave impedance is chosen to be $b = 1000$ Ns/m then the displayed mass is already increased to $m_t = 100$ kg.

12.4.2 Communication Induced Stiffness Reduction

If the environment exhibits spring characteristics a substantially reduced stiffness is displayed to the human. The environment feels softer than it really is. The displayed

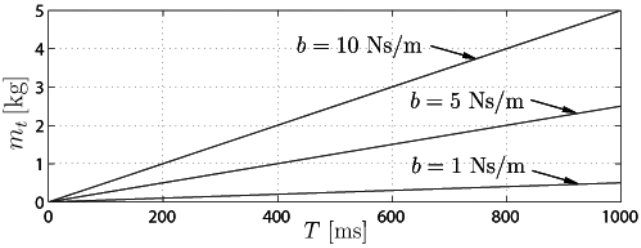

Fig. 12.4. Displayed inertia m_t in *free space motion* depending on round-trip time delay T and wave impedance b

stiffness coefficient (12.12) nonlinearly depends on the communication time delay as shown in Fig. 12.5 for different environment stiffness values. Ideal transparency in the sense of (12.1), i.e. $k_t = k_e$, is not achievable for non-zero time delay. Considering the human haptic perception limits, however, a transparency degradation should not be perceivable if the displayed stiffness is within the JND range of the environment stiffness $k_t > (1 - \text{JND}_k)k_e$ with $0 < \text{JND}_k < 1$ the stiffness JND. Accordingly, a stiff environment appears transparent to the human even for non-zero round-trip time delay as long as it satisfies

$$T < \frac{\text{JND}_k}{1 - \text{JND}_k} \frac{2b}{k_e} \tag{12.13}$$

which follows from inserting (12.12) in the previous equation. Note, that increasing environment stiffness reduces the allowable time delay margin. In contrast, a high value of the wave impedance b increases the delay margin, and reduces the impact of the time delay on stiffness reduction as observable from (12.12), i.e. increases the transparency of stiff environments. This, however, contradicts the design rule for free space motion. Good transparency in free space motion and for arbitrary stiff environments is not achievable at the same time.

Example 2. Consider a stiff wall with $k_e = 30000$ N/m, and the wave impedance tuned to $b = 1$ Ns/m. Already a very small round-trip delay of $T = 1$ ms substantially decreases the displayed stiffness to $k_t = 1875$ N/m, a reduction by 94%. At a delay of $T = 200$ ms the operator perceives only a stiffness of $k_t = 10$ N/m, hence 0.03% of the environment stiffness. Contacting a soft environment with $k_e = 10$ N/m, see Fig. 12.5, the displayed stiffness at $T = 1$ ms is still $k_t = 9.95$ N/m, at $T = 200$ ms still $k_t = 5$ N/m. Increasing the wave impedance for the hard wall to $b = 1000$ Ns/m at $T = 200$ ms the displayed stiffness is $k_t = 7500$N/m. Note the increased inertia in free space from the previous example with these values.

12.4.3 Communication Induced Stiffness Bound

The displayed stiffness (12.12) cannot exceed

$$k_{t,\max} = \lim_{k_e \to \infty} k_t = \frac{2b}{T}. \tag{12.14}$$

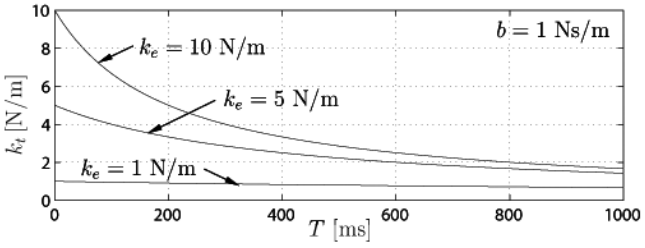

Fig. 12.5. Displayed stiffness k_t in *contact with a stiff wall* depending on round-trip time delay T and environment stiffness k_e

This result is also indicated by the asymptotic behavior of the displayed stiffness for increasing environment stiffness shown for a simulation example in Fig. 12.6. Considering the psychophysical fact that the human feels a wall to be rigid for $k_t \geq 24200$ N/m [35] it becomes clear that only for a very small time delay and a very large wave impedance b a rigid wall can be realistically displayed with this control architecture. For large time delay the stiffness, especially in case of hard walls, is not transparent. Appropriate tuning (high values) of the wave impedance b increases the transparency in terms of the maximum displayable stiffness.

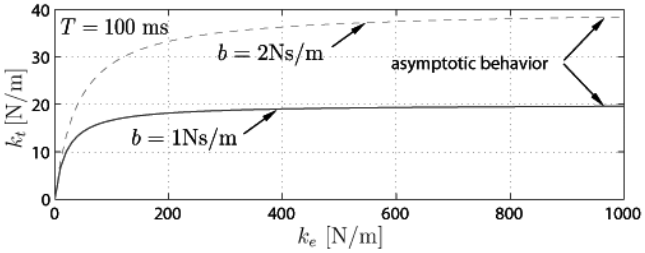

Fig. 12.6. Displayed stiffness k_t depending on environment stiffness k_e and wave impedance b

Example 3. Assuming a communication delay $T = 200$ ms with a wave impedance tuned to $b = 1$ Ns/m the maximum displayable stiffness is only $k_{h,max} = 10$ N/m. Any stiff environment feels very soft.

12.4.4 Bounded Displayable Stiffness Difference

In some tasks not only the absolute value of the displayed stiffness is important but also the possibility to distinguish between various stiff environments. This is especially important for e.g. tele-surgery applications, where different characteristics have to be distinguished. As indicated by the asymptotic behavior of the displayed stiffness in Fig. 12.6 at higher values of the environment stiffness, a stiffness difference in the environment results in a smaller difference in the displayed stiffness. However, a difference

between a reference value k_e^0 and a value k_e of the environment stiffness is perceivable by the human only if the corresponding percentual difference in the displayed stiffness

$$\delta k_t = |k_t - k_t^0|/k_t^0 \tag{12.15}$$

is larger than the stiffness JND

$$\delta k_t = \frac{2b\delta k_e}{2b + Tk_e} \geq \text{JND}_k \tag{12.16}$$

with the percentual difference in the environment stiffness δk_e defined analogously to (12.15) and the displayed reference stiffness $k_t^0 = k_t(k_e^0)$ according to (12.12). The percentual difference δk_t of the displayed stiffness and the environment stiffness δk_e is equal only for the marginal cases of zero delay $T = 0$ or infinite wave impedance $b \to \infty$. At high delay and high environment stiffness, a large difference in the environment stiffness may result in a non-perceivable difference of the displayed stiffness. According to (12.16) the appropriate tuning (high values) of the wave impedance b increases the transparency in terms of the range of environment stiffness where a difference is perceivable by the human.

Example 4. Let us assume a communication delay is $T = 200$ ms and the wave impedance tuned to $b = 1$ Ns/m. If the environment stiffness coefficient is $k_e > 40$ N/m than a difference to *any* larger environment stiffness is not perceivable under the 23%-JND assumption.

12.4.5 Just Noticeable Difference for Time Delay

So far the distortion induced by the absolute value of the time delay has been investigated. This section discusses when a relative increase of the time delay can be perceived by the human operator. Assuming that the delay difference is haptically perceived only by the difference in the mechanical properties of the displayed impedance, the just noticeable difference for time delay can be derived from the results from Sec. 12.3.2 and the well known JND's for mechanical properties. This result is interesting with respect to the design of control architectures for telerobotic sytems over the Internet coping with time-varying delay, where data buffering strategies, as e.g. in [19], introduce additional delay. If the additional delay results in a distortion below the human perception threshold then no change in transparency should be perceived.

The inertia $m_t^0 = m_t(T^0)$, see (12.9), and the stiffness $k_t^0 = k_t(T^0)$, see (12.12), represent the displayed mechanical properties at the reference time delay T^0. An additional time delay $\Delta T = T - T^0 > 0$ results in a further increased displayed inertia in *free space motion* and further reduced displayed stiffness in *contact with a stiff wall*. The further distortion due to the time delay difference is just noticeable by the human if the corresponding percentual difference of the displayed mechanical property is equal to the JND

$$\text{(a)} \quad \delta m_t(T^0, \Delta T) = \text{JND}_m \qquad \text{(b)} \quad \delta k_t(T^0, \Delta T) = \text{JND}_k, \tag{12.17}$$

where δm_t denotes the percentual difference of the displayed inertia defined similar as δk_t in (12.15), and JND_m the inertia JND. The just noticeable time delay difference is

computed straightforwardly using (12.9) and (12.12) in (12.17)(a) and (b), respectively. In *free space motion* a time delay difference is expected to be just perceivable by the human if

$$\frac{\Delta T}{T^0} = \text{JND}_m. \tag{12.18}$$

Obviously, the just noticeable time delay difference in free space motion follows a linear law similar to Weber's law, see Sec. 12.2.2. In *contact with a stiff wall* a time delay difference is expected to be just perceivable by the human if

$$\frac{\Delta T}{T^0} = \frac{\text{JND}_k}{\text{JND}_k + 1}\Big(\frac{2b}{k_e T^0} + 1\Big). \tag{12.19}$$

In contrast to the free space motion case, the just noticeable time delay depends on the environment stiffness k_e, the wave impedance b and the reference time delay T^0. In both cases, the absolute just noticeable difference ΔT increases with the reference time delay. Accordingly, any additional time delay should be avoided in the haptic telerobotic system, especially if the reference time delay is small. At high reference time delay an additional delay may not further perceivably degrade transparency. In consequence, if buffering strategies in telerobotic systems with time varying delay induce an additional time delay below the just noticeable difference, then human perceived transparency is not further degraded. For further results on the influence of communication effects on transparency refer to [22].

Remark 2. For the transparency analysis in this chapter the environment is assumed to be constant. Dynamic transitions between different environments, e.g. from free space motion to contact with a stiff wall, also have an influence on the perceived transparency as indicated in [36]. The analysis requires different techniques and is beyond the scope of this chapter.

Remark 3. The displayed impedance parameters in (12.9) and (12.12) are derived for the wave (scattering) variable approach. Consequently, all results in (12.14), (12.16), (12.18), and (12.19) are valid only for this specific control architecture. A perception oriented transparency analysis of other control architectures is straightforward by using the corresponding expressions for the parameters of the displayed impedance, e.g. from [29].

12.5 Perception Oriented Design Aspects in Real Systems

The tuning of the wave impedance b has a high impact on the transparency of the communication subsystem as observed in the previous sections. The transparency criterion (12.1) requires for free space motion $b \to 0$ as observable from (12.9). In contact with a stiff environment, time delay has no influence on transparency if $b \to \infty$, see (12.12), (12.14), (12.16). These are contradicting design rules, that can be relaxed by considering human haptic perception and a real telerobotic system as shown in the following.

In real telerobotic systems with limited control input and robustly designed controllers the dynamics of the master and the slave device is generally not negligible.

As a result, even without time delay transparency in the sense of (12.1) is not achievable. In the following, master and slave dynamics refers to the locally controlled device dynamics.

In free space motion, at least the inertia m_m induced by the master dynamics is displayed to the human. If the wave impedance is chosen

$$b < \frac{2}{T}\text{JND}_m m_m, \tag{12.20}$$

then the displayed overall inertia, the sum of the master and the communication induced inertia, is within the JND range of the master inertia $m_t < (1 + \text{JND}_m)m_m$ as straightforward derivable from (12.9). No additional communication induced transparency degradation should be perceivable by the human then. The original design requirement $b \to 0$ is relaxed.

In order to avoid contact instability or oscillations, the slave device is typically compliance controlled. The resulting stiffness $k_{s/e}$ of the slave device together with the environment computes from the environment stiffness k_e and the stiffness k_s of the compliance controlled slave device according to the serial connection of springs $k_{s/e}^{-1} = k_e^{-1} + k_s^{-1}$. If the wave impedance is chosen to be

$$b > \frac{T}{2}(\text{JND}_k^{-1} - 1)k_{s/e}, \tag{12.21}$$

then the communication induced reduction is within the JND range of the combined slave device/environment stiffness $k_t > (1 - \text{JND}_k)k_{s/e}$. The upper bound of the slave device/environment stiffness $\sup_{k_e} k_{s/e} = \lim_{k_e \to \infty} k_{s/e} = k_s$, i.e. the slave device compliance, determines the lower bound of a transparently designed wave impedance b (12.21). Clearly, the original transparency requirements for the communication subsystem design $b \to \infty$ are relaxed by (12.21).

Example 5. The haptic input device ViSHaRD10 (see chapter 2) displays without time delay an inertia of at least $m_m = 8\,\text{kg}$. With a for the Internet realistic round-trip time delay of $T = 160\,\text{ms}$ and a inertia JND assumption of $\text{JND}_m = 21\%$ [27] for communication transparent design in free space motion the wave impedance should $b < 21\,\text{Ns/m}$ (12.20). In contact with a stiff wall, assuming a slave device compliance of $k_s = 900\,\text{N/m}$ as in [37] and a stiffness JND of 23% [25], the wave impedance should be $b > 241\,\text{Ns/m}$ (12.21). The gap between the design requirements for the wave impedance b for free space motion and contact with a stiff wall derived from the strict transparency criterion (12.1) become smaller by considering human perception aspects and the real telerobotic system.

12.6 Experiments

In the first experiment the dependency of the displayed impedance parameters on the round-trip time delay obtained in Sec. 12.3 by (12.9), (12.12) is validated. In the second one, a human user study is conducted on how a relative increase of time delay further degrades the human perceived transparency. In both experiments, the prototypical cases of *free space motion* and *contact with a stiff wall* (stiffness coefficient $k_e = 12.5\,\text{kN/m}$) are investigated.

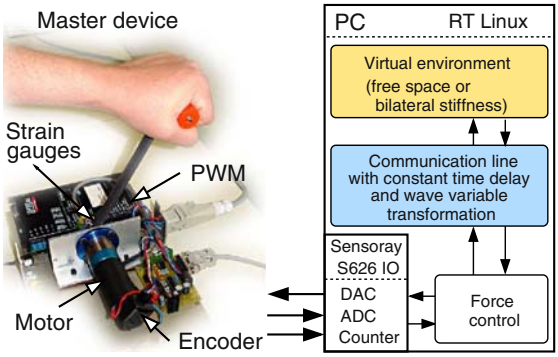

Fig. 12.7. Experimental system architecture with a 1DoF telerobotic system

12.6.1 Experimental Setup

The experimental setup, see Fig. 12.7, consists of a single degree-of-freedom force feedback paddle connected to a PC. The paddle DC motor torque is controlled by the PWM amplifier. The force applied to the paddle lever is measured by a strain gauge bridge, the position of the lever by an optic pulse incremental encoder. A virtual environment is used instead of a real slave device/environment in order to seperately consider the prototypical environment scenarios, especially in the human user studies. The virtual environment, the control loops, the model of the communication subsystem with different constant delay and the wave (scattering) variable transformation with a wave impedance $b = 125\,\text{Ns/m}$ are composed of MATLAB/SIMULINK blocksets; standalone realtime code for RT Linux is automatically generated from that. All experiments were performed with a sample time interval $T_A = 0.001\text{s}$.

12.6.2 Objective Measurements

The displayed inertia m_t in free space motion and the displayed stiffness k_h in contact with the wall are determined depending on the round-trip time delay that is varied within the interval $T \in [5,\ 400]$ ms. The parameters m_t and k_t are determined by a least squares identification from the measured slave position and slave force signals. The results for the displayed inertia in free space motion are shown in Fig. 12.8 (a) [1], and for the displayed stiffness in contact in Fig. 12.8 (b). The theoretically obtained dependencies of these parameters on the round-trip time delay given by (12.9) and (12.12) are convincingly validated. The slightly reduced stiffness and the higher inertia in the experiments result from the limited bandwidth of the conservatively tuned force control loop at the slave.

12.6.3 Human User Study

The hypothesis to be validated is that at low reference time delay the relative time delay increase detection threshold is smaller than at high reference time delay, see Sec. 12.4.5.

[1] The inertia results for $T < 100$ ms are missing because of numerical unreliabilities in the least squares estimation.

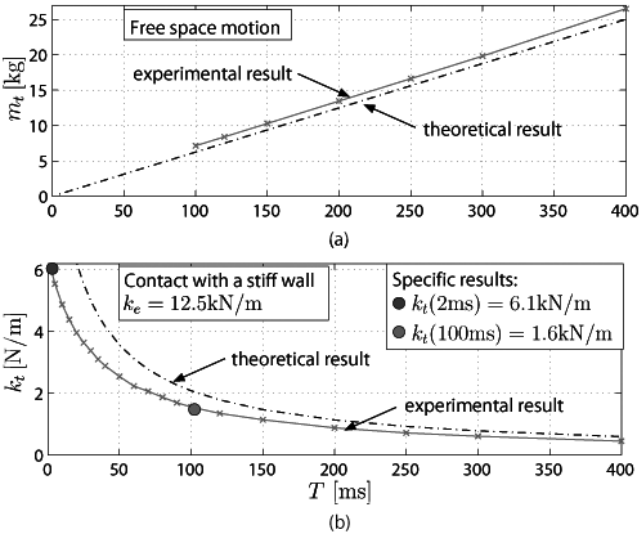

Fig. 12.8. Experimentally obtained displayed inertia m_t (a) and stiffness k_t (b) depending on round-trip delay T compared to theoretical results

Four experiments with 7 subjects (aged 20–30, 3 female, 4 male) were performed for two different reference round-trip time delays $T^0 = 2\,\text{ms}$ and $T^0 = 100\,\text{ms}$ for each of the considered prototypical cases *free space motion* and *contact with a wall* using the same parameters as in the foregoing experiment. The subjects were told to operate with their preferred hand. They were equipped with earphones to mask the sound the device motors generate. No visual feedback of the virtual environment was provided. The subjects were not refunded. During a familiarization phase subjects were told to feel operation for the reference round-trip delay configuration. As soon as they felt familiar with the system the measurement phase began.

12.6.4 Procedure

In order to determine the detection thresholds for the time delay difference the three interval forced choice (3IFC) paradigm has been applied, which is a common experimental tool in psychophysics to determine detection thresholds in human haptic perception [30]. The main feature is that the subjects are presented three consecutive time intervals, 20s duration each, two with the reference value T^0 of the time delay, one - randomly chosen which - with a different time delay value T. The subject has to tell which of the intervals felt different. Starting from a non-perceivable delay difference ΔT this value is increased after every incorrect answer until three consecutive correct answers on the same value ΔT are given. No feedback on the correctness of the answer was given. Three of these passes are performed, the mean value over the passes is considered the subject specific discrimination threshold. The experiment started with a delay of $T_{2\text{ms}} = 3\,\text{ms}$ ($T_{100\text{ms}} = 103\,\text{ms}$), i.e. a delay difference

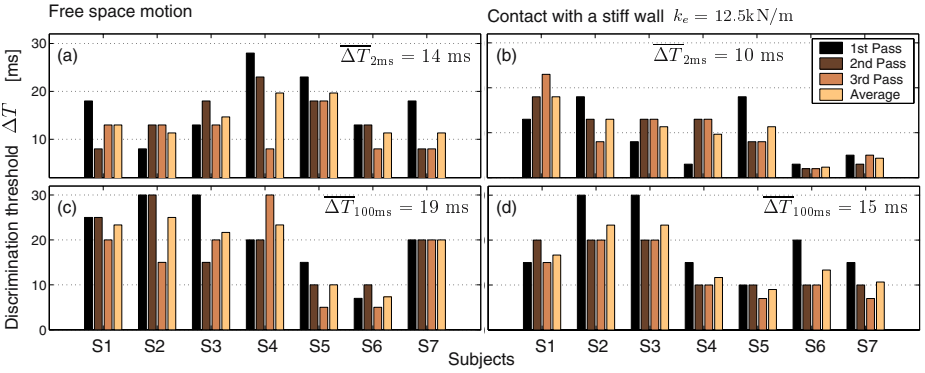

Fig. 12.9. Results of human user study: discrimination thresholds for time delay ΔT at reference time delays $T_0 = 2$ ms (a), (b) and $T_0 = 100$ ms (c), (d) for free space motion (a), (c) and contact with a stiff wall (b), (d)

Table 12.2. Results of human user study: Average detected delay differences and corresponding percentual parameter differences for different reference time delays T_0

	Free space $T_0 = 2$ms	Free space $T_0 = 100$ms	Contact $T_0 = 2$ms	Contact $T_0 = 100$ms
$\overline{\Delta T}$ [ms]	14	19	10	15
$\lvert m_t^0 - m_t \rvert$ [kg]	n.a.[1]	0.048		
δm_t [%]	n.a.[1]	17		
$\lvert k_t^0 - k_t \rvert$ [kN]			1.2	0.16
δk_t [%]			20	10

of $\Delta T_{2\mathrm{ms}} = 1$ ms ($\Delta T_{100\mathrm{ms}} = 3$ ms), where values $(\cdot)_{2\mathrm{ms}}$ indicate a reference round-trip delay of $T_0 = 2$ ms, and accordingly $(\cdot)_{100\mathrm{ms}}$ refers to $T_0 = 100$ ms.

Results

The results for all four experiments are shown in Fig. 12.9, where $\overline{\Delta T}$ denotes the average over all subjects, see also the first row in Table 12.2. As expected from the theoretical results in Sec. 12.4.5, in both scenarios, the average detected delay difference is smaller for low reference time delay $\overline{\Delta T}_{2\mathrm{ms}} < \overline{\Delta T}_{100\mathrm{ms}}$. The Student's test is performed giving a statement about the statistical significance of the discrimination thresholds difference $(\Delta T_{2\mathrm{ms}} - \Delta T_{100\mathrm{ms}})$. Even with this rather small number of subjects, for *contact with a stiff wall* the mean discrimination threshold for low reference delay is statistically significant (95%) smaller than for high reference delay. For *free space motion* it is not significant (90%) in a statistical sense: As expected time delay is more crucial for the transparency degradation in very stiff environments. For a cross check the percentual differences (12.15) of the displayed inertia δm_t and stiffness δk_t corresponding to these just noticeable time delay differences are computed using the results from the previous experiment. For example, the average discrimination threshold $\overline{\Delta T}_{2\mathrm{ms}} = 10$ ms for

contact with a stiff wall corresponds to a percentual difference in the displayed stiffness of $\delta k_{h,2\text{ms}} = 20\,\%$. The percentual differences, see Table 12.2[2], are all in the range of the JNDs reported in literature (for stiffness: 8% [26], $(23 \pm 3)\%$ [25], for inertia $(21 \pm 3.5)\%$ [27]), see also Table 12.1 for comparison.

In summary, the results indicate, that the discrimination threshold for time delay is lower for low round-trip delay as predicted in Sec. 12.4.5. Accordingly, any additional time delay should be avoided if the communication delay is very low. For high communication delay some additional delay does not further degrade human perceived transparency.

12.7 Conclusions

The consideration of human factors is important for the design and evaluation of telerobotic systems. In this chapter a method for the transparency analysis of haptic telerobotic systems is presented with the goal to quantify the degradation induced by communication time delay from a human perception point of view. Therefore the effect of constant time delay and of the wave (scattering) variable control approach on the mechanical properties displayed to the human is analyzed. The interpretation of the results using known psychophysical facts reveals important insights with implications for the control design and the range of tele-applications depending on the communication time delay: a) in free space motion time delay introduces artificial inertia; b) stiff environments are perceived softer; c) displayable stiffness is upper bounded; d) environment stiffness discrimination is limited; e) there is a detection threshold for relative changes in time delay. Nevertheless, ideal transparency requiring the displayed impedance to be exactly equal to the environment impedance is not necessary for the telerobotic system to be perceived transparent by the human. The consideration of human haptic perception limits leads to relaxed design requirements still guaranteeing human perceived transparency. Psychophysically motivated design guidelines for the wave impedance as well as upper time delay bounds for human perceived transparency are derived in this chapter. The just noticeable difference for time delay gives implications for the design of telerobotic systems with time-varying delay. The obtained results are validated in experiments and human user studies.

The approach in this chapter constitutes a first step towards a human perception oriented analysis of the time delay on the transparency. Exciting challenges incorporate the systematic human perception oriented transparency analysis of general communication unreliabilities, and a rigorous human perception oriented design of multimodal, multi-DoF telerobotic systems.

Acknowledgements

This work is supported in part by the DFG Collaborative Research Center SFB453 and the Technische Universität München.

[2] As the inertia for $T_0 = 2\,\text{ms}$ could not be identified from the sensor signals in the foregoing experiment, the corresponding percentual difference in inertia not available (n.a.) in Table 12.2.

References

1. W.R. Ferrell. Remote Manipulation with Transmission Delay. *IEEE Transactions on Human Factors*, 6:24–32, 1965.
2. R.J. Anderson and M.W. Spong. Bilateral Control of Teleoperators with Time Delay. *IEEE Transactions on Automatic Control*, 34(5):494–501, 1989.
3. G. Niemeyer and J.-J.E. Slotine. Stable Adaptive Teleoperation. *IEEE Journal of Oceanic Engineering*, 16(1):152–162, January 1991.
4. G.J. Raju, G.C. Verghese, and T.B. Sheridan. Design Issues in 2-Port Network Models of Bilateral Remote Teleoperation. In *Proceedings of the IEEE International Conference on Robotics and Automation*, pages 1317–1321, Scottsdale (AZ), US, 1989.
5. D.A. Lawrence. Stability and Transparency in Bilateral Teleoperation. *IEEE Transactions on Robotics and Automation*, 9(5):624–637, October 1993.
6. Y. Yokokohji and T. Yoshikawa. Bilateral Control of Master-Slave Manipulators for Ideal Kinesthetic Coupling Formulation and Experiment. *IEEE Transactions on Robotics and Automation*, 10(5):605–619, 1994.
7. B. Hannaford. Stability and Performance Tradeoffs in Bi-Lateral Telemanipulation. In *Proceedings of the IEEE International Conference on Robotics and Automation*, pages 1764–1767, Scottsdale (AZ), US, 1989.
8. K. Hashtrudi-Zaad and S.E. Salcudean. Analysis and Evaluation of Stability and Performance Robustness for Teleoperation Control Architectures. In *Proc. of the IEEE Int. Conf. on Robotics and Automation*, pages 3107–3113, San Francisco (CA), US, 2000.
9. J. Vertut, A. Micaelli, P. Marchal, and J. Guittet. Short Transmission Delay on a Force Reflective Bilateral Manipulator. In *Proceedings of the 4th Rom-An-Sy*, pages 269–274, Zaborow, Poland, 1981.
10. C.A. Lawn and B. Hannaford. Performance Testing of Passive Communication and Control in Teleoperation with Time Delay. In *Proceedings of the IEEE International Conference on Robotics and Automation*, pages 776–783, Atlanta (GA), US, 1993.
11. G. Hirzinger. ROTEX–The First Robot in Space. In *Proceedings of the ICAR International Conference on Advanced Robotics*, pages 9–33, Tokyo, Japan, 1993.
12. G. Niemeyer and J. E. Slotine. Towards Force-Reflecting Teleoperation Over the Internet. In *Proceedings of the IEEE International Conference on Robotics and Automation*, pages 1909–1915, Leuven, Belgium, 1998.
13. R. Lozano, N. Chopra, and M. Spong. Passivation of Force Reflecting Bilateral Teleoperators with Time Varying Delay. In *Proceedings of the 8. Mechatronics Forum*, pages 954–962, Enschede, Netherlands, 2002.
14. N. Chopra, M.W. Spong, S. Hirche, and M. Buss. Bilateral Teleoperation over Internet: the Time Varying Delay Problem. In *Proceedings of the American Control Conference*, pages 155–160, Denver (CO), US, 2003.
15. Y. Yokokohji, T. Imaida, and T. Yoshikawa. Bilateral Control with Energy Balance Monitoring under Time-Varying Communication Delay. In *Proceedings of the IEEE International Conference on Robotics and Automation*, pages 2684–2689, San Francisco (CA), US, 2000.
16. S. Munir and W.J. Book. Internet Based Teleoperation using Wave Variable with Prediction. *ASME/IEEE Transactions on Mechatronics*, 7(2):124–133, 2002.
17. S. Stramigioli. About the Use of Port Concepts for Passive Geometric Telemanipulation with Time Varying Delays. In *Proceedings of the 8. Mechatronics Forum*, pages 944–953, Enschede, The Netherlands, 2002.
18. Y. Yokokohji, T. Tsujioka, and T. Yoshikawa. Bilateral Control with Time-Varying Delay including Communication Blackout. In *Proceedings of the 10th Symposium on Haptic Interfaces for Virtual Environment and Teleoperator Systems*, Orlando (FL), US, 2002.

19. B. Berestesky, N. Chopra, and M. W. Spong. Discrete Time Passivity in Bilateral Teleoperation over the Internet. In *Proceedings of the IEEE International Conference on Robotics and Automation ICRA'04*, pages 4557–4564, New Orleans, US, 2004.
20. S. Hirche and M. Buss. Packet Loss Effects in Passive Telepresence Systems. In *Proceedings of the 43rd IEEE Conference on Decision and Control*, pages 4010–4015, Paradise Island, Bahamas, 2004.
21. C. Secchi, S. Stramigioli, and C. Fantuzzi. Dealing with Unreliabilities in Digital Passive Geometric Telemanipulation. In *Proceedings of the IEEE/RSJ International Conference on Intelligent Robots and Systems IROS*, Las Vegas (NV), US, 2003.
22. S. Hirche. *Haptic Telepresence in Packet Switched Communication Networks*. PhD thesis, Technische Universität München, Institute of Automatic Control Engineering, July 2005.
23. X. Wang, P.X. Liu, D. Wang, B. Chebbi, and M. Meng. Design of Bilateral Teleoperators for Soft Environments with Adaptive Environmental Impedance Estimation. In *Proceedings of the IEEE International Conference on Robotics and Automation*, pages 1139–1144, Barcelona, Spain, 2005.
24. K. Hashtrudi-Zaad and S.E. Salcudean. Analysis of Control Architectures for Teleoperation Systems with Impedance/Admittance Master and Slave Manipulators. *International Journal of Robotics Research*, 20(6):419–445, 2001.
25. L.A. Jones and I.W. Hunter. A Perceptual Analysis of Stiffness. *Experimental Brain Research*, 79:150–156, 1990.
26. H.Z. Tan, N.I. Durlach, G.L. Beauregard, and M.A. Srinivasan. Manual Discrimination of Compliance Using Active Pinch Grasp: The Role of Force and Work Cues. *Perception and Psychophysics*, 57:495–510, 1995.
27. G.L. Beauregard and M.A. Srinivasan. The Manual Resolution of Viscosity and Mass. *ASME Dynamic Systems and Control Division*, 1:657–662, 1995.
28. L.A. Jones and I.W. Hunter. A Perceptual Analysis of Viscosity. *Experimental Brain Research*, 94(2):343–351, 1993.
29. P. Arcara and C. Melchiorri. Control Schemes for Teleoperation with Time Delay: A Comparative Study. *Robotics and Autonomous Systems*, 38(1):49–64, 2002.
30. G.A. Gescheider. *Psychophysics: The Fundamentals*. Lawrence Erlbaum and Associates, 3rd Edition, Hillsdale, 1997.
31. G.C. Burdea. *Force and Touch Feedback for Virtual Reality*. John Wiley, 1996.
32. E. H. Weber. *Die Lehre vom Tastsinn und Gemeingefühl, auf Versuche gegründet*. Vieweg, 1851.
33. L. A. Jones and I. W. Hunter. Human Operator Perception of Mechanical Variables and Their Effects on Tracking Performance. *ASME Advances in Robotics*, 42:49–53, 1992.
34. G. Niemeyer and J.-J.E. Slotine. Telemanipulation with Time Delays. *International Journal of Robotic Research*, 23(9):873–890, September 2004.
35. H.Z. Tan, M.A. Srinivasan, B. Eberman, and B. Cheng. Human Factors for the Design of Force-Reflecting Haptic Interfaces. *ASME Dynamic Systems and Control Division*, 1:353–359, 1994.
36. N.A. Tanner and G. Niemeyer. Improving Perception in Time Delayed Telerobotics. *International Journal of Robotics Research*, 2005.
37. B. Stanczyk and M. Buss. Experimental comparison of interaction control methods for a redundant telemanipulator. In *Proceedings of the International Symposium on Methods and Models in Automation and Robotics MMAR'2005*, pages 677–682, Poland, 2005.